LM-PIELM: Hard Constraint Enforcement in Physics-Informed Extreme Learning Machines

A Lagrange-Multiplier Framework for PDE-Governed Forward and Inverse Problems

Authors: Eshan Kulkarni, Rishi Mishra, Balaji Srinivasan

Accepted at the ICML 2026 Workshop on AI for Physics

Motivation and Problem Statement

Traditional solvers (FEM/FDM)

✅ Accurate and Physically consistent
❌ Expensive meshes, difficult for complex gemetries

↓

PINNs

✅ Mesh-free and flexible
❌ Slow, non-convex optimization, soft BC enforcement

↓

PIELMs

✅ Fast linear solve, more stable
❌ soft BC enforcement

Soft Boundary enforcement:

$$\mathcal{L} = \mathcal{L}_{PDE} + \mu_{BC}\mathcal{L}_{BC}$$

- Requires manual tuning of penalty weights
- Poor balance between PDE residual and BC satisfaction
- Can become unstable in stiff/advection-dominated PDEs

Can boundary conditions be enforced exactly rather than approximately?

Literature Landscape and Research Gap

TFC/X-TFC

- TFC constructs constrained expressions in which the admissible solution space is analytically parameterized
- X-TFC combines TFC constrained expressions with Extreme Learning Machine (ELM) architecture
- Excellent accuracy and stability across several benchmark PDE problems
- Boundary admissibility is preserved independently of optimization dynamics or loss balancing
- Constrained expressions need to be derived separately for each problem class, gemoetry and configuration

AL-PINNs

- Introduce Lagrange multipliers into the PINN training objective in order to improve constraint satisfaction
- Boundary constraints coupled to the optimization process through dual variables and iteratively updated
- Improves convergence behaviour, reduces sensitivity to penalty-weight selection as compared to soft-penalty
- Resulting optimization process is non-linear and non-convex and requires iterative updation
- AL-PINNs still require stabilization penalties, tuning parameters to ensure robust convergence

The Gap that LM-PIELM fills

- Eliminates penalty tuning, exact BC enforcement, linear solvability, and geometry-agnostic flexibility
- Extends naturally to the class of Inverse Problems, maintaining exact BC enforcement irrespective of interior loss

LM-PIELM: From soft constraints to hard constraints

Conventional PIELM

$$\min_{\mathbf{C}} \frac{1}{2}\|\boldsymbol{\Psi}\mathbf{C} - \mathbf{f}\|_2^2 + \frac{\mu_{BC}}{2}\|\boldsymbol{\Phi}_b\mathbf{C} - \mathbf{g}\|_2^2$$

- Boundary conditions enforced approximately
- Requires tuning of the penalty parameter
- Trade-off between PDE accuracy and BC satisfaction

LM-PIELM

$$\min_{\mathbf{C}} \frac{1}{2}\|\boldsymbol{\Psi}\mathbf{C} - \mathbf{f}\|_2^2 \quad \text{subject to} \quad \boldsymbol{\Phi}_b\mathbf{C} = \mathbf{g}$$

- Exact constraint enforcement
- No penalty parameter tuning
- Constraints remain decoupled from the PDE residual

In LM-PIELM formulation, boundary conditions become part of the solution space, not merely optimization penalties. We replace optimization penalties with algebraic constraints

LM-PIELM Formulation

Equality-Constrained Problem

$$\min_{\mathbf{C}} \frac{1}{2}\|\Psi\mathbf{C} - \mathbf{f}\|_2^2$$

$$\text{subject to } \Phi_b\mathbf{C} = \mathbf{g}$$

Minimize PDE residual while satisfying BCs exactly

Introduce Lagrange Multipliers

$$\mathcal{L}(\mathbf{C}, \boldsymbol{\lambda}) = \frac{1}{2}\|\Psi\mathbf{C} - \mathbf{f}\|_2^2 + \boldsymbol{\lambda}^\top(\Phi_b\mathbf{C} - \mathbf{g})$$

λ enforces algebraic constraints

Linear Saddle-Point system

$$\underbrace{\begin{bmatrix} \Psi^\top\Psi & \Phi_b^\top \\ \Phi_b & 0 \end{bmatrix}}_{\mathbf{K}} \begin{bmatrix} \mathbf{C} \\ \boldsymbol{\lambda} \end{bmatrix} = \begin{bmatrix} \Psi^\top\mathbf{f} \\ \mathbf{g} \end{bmatrix}$$

- Fully linear constrained solve
- Mixed BCs and ICs handled uniformly

Augmented-system LM-PIELM

Improving numerical robustness

Reduced Formulation

$$\underbrace{\begin{bmatrix} \Psi^\top \Psi & \Phi_b^\top \\ \Phi_b & 0 \end{bmatrix}}_{\mathbf{K}} \begin{bmatrix} \mathbf{C} \\ \boldsymbol{\lambda} \end{bmatrix} = \begin{bmatrix} \Psi^\top \mathbf{f} \\ \mathbf{g} \end{bmatrix}$$

- Requires forming $\Psi^\top \Psi$
- Can amplify conditioning issues
- Instability in stiff/advection-dominated problems

$$\mathcal{L}(\mathbf{C}, \boldsymbol{\lambda}) = \frac{1}{2}\|\Psi\mathbf{C} - \mathbf{f}\|_2^2 + \boldsymbol{\lambda}^\top(\Phi_b\mathbf{C} - \mathbf{g})$$

Introduce residual variable

$$\mathbf{r} = \Psi\mathbf{C} - \mathbf{f}$$

Augmented-System Formulation

$$\underbrace{\begin{bmatrix} I_{N_c} & -\Psi & 0 \\ \Psi^\top & 0 & \Phi_b^\top \\ 0 & \Phi_b & 0 \end{bmatrix}}_{\mathbf{K}_{\text{aug}}} \begin{bmatrix} \mathbf{r} \\ \mathbf{C} \\ \boldsymbol{\lambda} \end{bmatrix} = \begin{bmatrix} -\mathbf{f} \\ \mathbf{0} \\ \mathbf{g} \end{bmatrix}$$

- Avoids explicit construction of $\Psi^\top \Psi$
- Better numerical conditioning
- Improved robustness in difficult PDEs
- Maintains mathematical equivalence

$$\mathcal{L}(\mathbf{r}, \mathbf{C}, \boldsymbol{\gamma}, \boldsymbol{\lambda}) = \frac{1}{2}\mathbf{r}^\top\mathbf{r} + \boldsymbol{\gamma}^\top(\mathbf{r} - \Psi\mathbf{C} + \mathbf{f}) + \boldsymbol{\lambda}^\top(\Phi_b\mathbf{C} - \mathbf{g})$$

Inverse Problems: Formulation and Theory

Parameter identification

$$\min_{\mathbf{C}} \frac{1}{2}\|\Psi(\theta)\mathbf{C} - \mathbf{f}\|_2^2 + \frac{1}{2}\|S\mathbf{C} - \mathbf{d}\|_2^2$$

$$\text{subject to} \quad \Phi_b\mathbf{C} = \mathbf{g}$$

- To find an unknown scalar parameter enters the PDE operator
- S is the sensor evaluation matrix, d are the measurements (with gaussian noise) at the locations

$$\begin{bmatrix} \Psi(\theta)^\top\Psi(\theta) + S^\top S & \Phi_b^\top \\ \Phi_b & 0 \end{bmatrix} \begin{bmatrix} \mathbf{C} \\ \boldsymbol{\lambda} \end{bmatrix} = \begin{bmatrix} \Psi(\theta)^\top\mathbf{f} + S^\top\mathbf{d} \\ \mathbf{g} \end{bmatrix}$$

Reduced form to Augmented form

$$\begin{bmatrix} I & -A_\theta & 0 \\ A_\theta^\top & 0 & \Phi_b^\top \\ 0 & \Phi_b & 0 \end{bmatrix} \begin{bmatrix} \mathbf{r}_\theta \\ \mathbf{C} \\ \boldsymbol{\lambda} \end{bmatrix} = \begin{bmatrix} -\mathbf{b}_\theta \\ \mathbf{0} \\ \mathbf{g} \end{bmatrix} \quad A_\theta = \begin{bmatrix} \Psi(\theta) \\ S \end{bmatrix}, \quad \mathbf{b}_\theta = \begin{bmatrix} \mathbf{f} \\ \mathbf{d} \end{bmatrix}$$

Source Recovery

$$\min_{\mathbf{C}} \frac{1}{2}\|S\mathbf{C} - \mathbf{d}\|_2^2 + \frac{\beta}{2}\|\mathbf{C}\|_2^2$$

$$\text{subject to} \quad \Phi_b\mathbf{C} = \mathbf{g}$$

- Forcing term is unknown and must be inferred from measurements of the solution
- Nomenclature for S & d is same, while beta is the Tikhonov regulariser used to improve conditioning

$$\begin{bmatrix} S^\top S + \beta I & \Phi_b^\top \\ \Phi_b & 0 \end{bmatrix} \begin{bmatrix} \mathbf{C} \\ \boldsymbol{\lambda} \end{bmatrix} = \begin{bmatrix} S^\top\mathbf{d} \\ \mathbf{g} \end{bmatrix}$$

Reduced form to Augmented form

$$\begin{bmatrix} I & -A_\beta & 0 \\ A_\beta^\top & 0 & \Phi_b^\top \\ 0 & \Phi_b & 0 \end{bmatrix} \begin{bmatrix} \mathbf{r}_\beta \\ \mathbf{C} \\ \boldsymbol{\lambda} \end{bmatrix} = \begin{bmatrix} -\mathbf{b}_\beta \\ \mathbf{0} \\ \mathbf{g} \end{bmatrix} \quad A_\beta = \begin{bmatrix} S \\ \sqrt{\beta} I \end{bmatrix}, \quad \mathbf{b}_\beta = \begin{bmatrix} \mathbf{d} \\ \mathbf{0} \end{bmatrix}$$

Results and Discussion

Forward Problems

Steady 1D Advection-Diffusion equation

$$u_x - \nu u_{xx} = f(x), \quad u(0) = 0, \quad u(1) = 1.$$

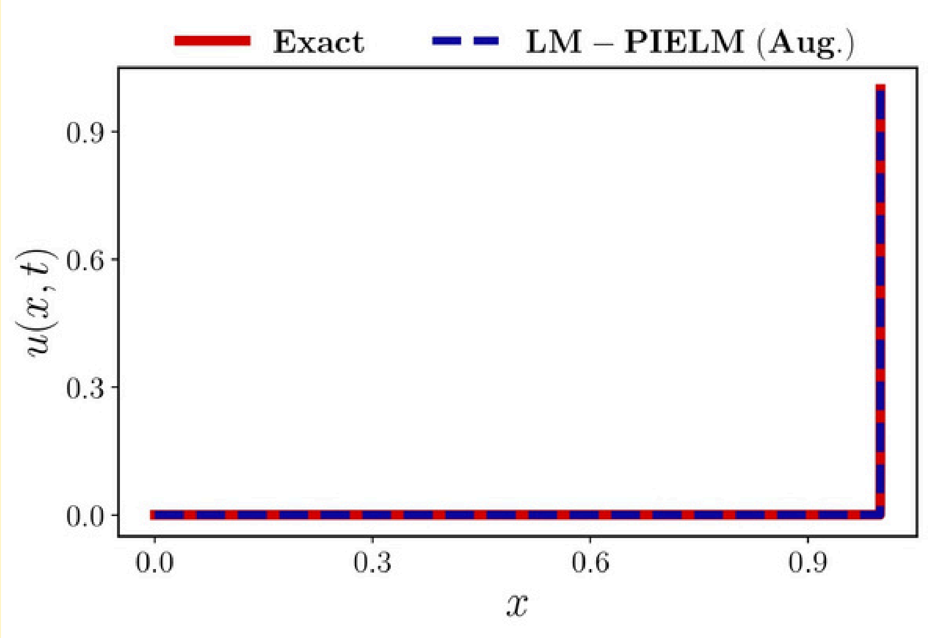

LM-PIELM (Aug.) solution for ν = 0.0001

ν	Method	$\lVert u_{ex} - \hat{u} \rVert_\infty$	$\lVert \Phi_b C - g \rVert_\infty$
0.01	X-TFC	1.73×10^{-12}	Exact
	PIELM	2.18×10^{-8}	2.18×10^{-8}
	LM-PIELM	1.87×10^{-14}	2.22×10^{-16}
	LM-PIELM (Aug.)	$\mathbf{1.27 \times 10^{-14}}$	$\mathbf{2.21 \times 10^{-16}}$
0.001	X-TFC	2.83×10^{-12}	Exact
	PIELM	4.89×10^{-5}	4.89×10^{-5}
	LM-PIELM	4.04×10^{-11}	6.66×10^{-16}
	LM-PIELM (Aug.)	$\mathbf{9.34 \times 10^{-13}}$	$\mathbf{2.22 \times 10^{-16}}$
0.0001	X-TFC	2.89×10^{-3}	Exact
	PIELM	5×10^{-1}	4.89×10^{-1}
	LM-PIELM	7.17×10^{-2}	1.78×10^{-5}
	LM-PIELM (Aug.)	$\mathbf{1.61 \times 10^{-4}}$	$\mathbf{9.31 \times 10^{-14}}$

Comparison table with L_infinity errors at interior and boundary for different values of ν

Configurations (N, Nc)

100, 1500

1200, 2500

3500, 7000

N = no. of basis, Nc = collocation points

- For ν = 0.01, both LM-PIELM formulations give solution errors of order 10^{-14} with BC residual at machine precision
- At ν = 0.0001, X-TFC and standard PIELM both exhibit noticeable degradation in solution accuracy, with standard PIELM additionally showing substantial boundary-condition errors due to the soft-penalty formulation
- The reduced LM-PIELM formulation improves over PIELM with a boundary residual of order 10^{-5}, while augmented achieves a substantially lower solution error than all other methods, maintaining boundary residual at order of 10^{-14}
- Although, the wall clock-time goes up to 29 s for the augmented formulation, the improved robustness and accuracy for lower values of ν indicate a favourable trade-off when numerical conditioning becomes a dominant concern

2D Poisson Equation with Mixed Boundary Conditions

$$u_{xx} + u_{yy} = f(x,y), \quad \Omega = (0,1)^2, \quad u_{\text{ex}}(x,y) = y^2 \sin(\pi x), \quad \frac{\partial u}{\partial y}(x,1) = 2\sin(\pi x), \text{ Dirichlet conditions on rest of the 3 sides}$$

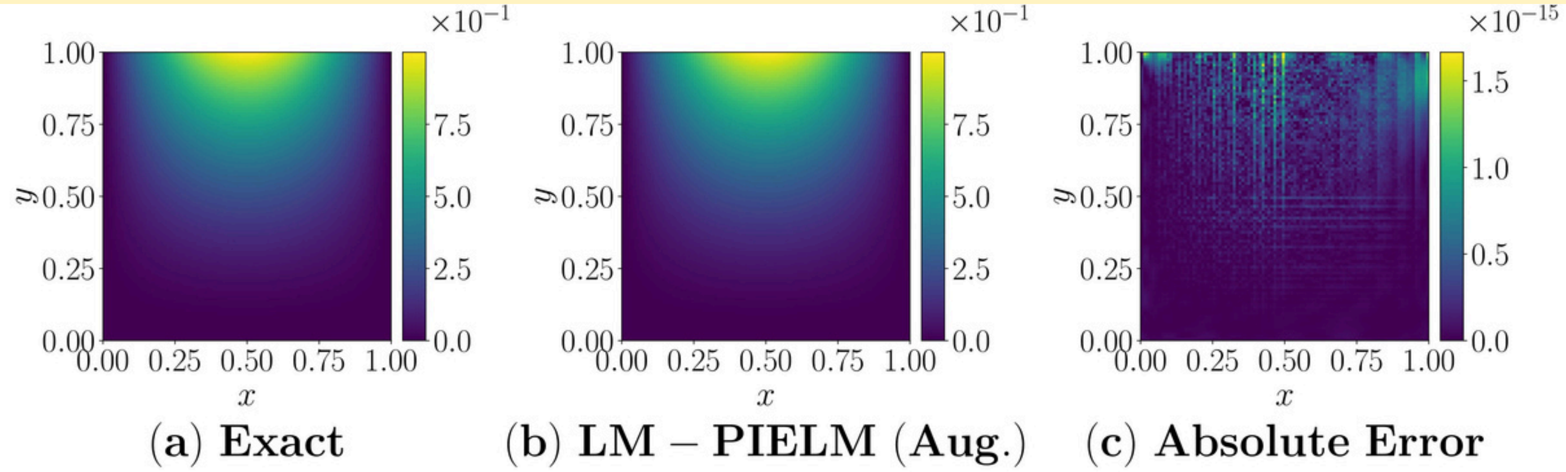

LM-PIELM (Aug.) solution plots

Configurations (N, Nc, Nb) = (289, 2304, 196)

Case	Method	$\|u_{\text{ex}} - \hat{u}\|_\infty$	$\|\Phi_b \mathbf{C} - \mathbf{g}\|_\infty$
Mixed BC	X-TFC	7.58×10^{-12}	Exact
	PIELM	1.78×10^{-10}	1.68×10^{-9}
	LM-PIELM	2.79×10^{-12}	5.61×10^{-13}
	LM-PIELM (Aug.)	$\mathbf{1.67 \times 10^{-15}}$	$\mathbf{6.51 \times 10^{-15}}$

Comparison table across different frameworks

- In conventional soft-penalty formulations, mixed boundary conditions often require careful balancing between separate residual terms corresponding to Dirichlet and Neumann operators
- PIELM produces relatively small solution errors, but the boundary residual remains several orders of magnitude larger than those obtained with the constrained formulations
- X-TFC serves as an important reference for hard-constrained behaviour in this case
- Both LM-PIELM formulations significantly improve the discrete boundary enforcement and maintains very high solution accuracy, while LM-PIELM (Aug.) reaching near machine precision for both solution and BC errors
- The absence of localized degradation near the Neumann boundary demonstrates that Dirichlet and Neumann operators can be enforced simultaneously without requiring separate tuning parameters or specialized treatment.

2D Poisson Equation with Star-shaped Domain

$$u_{xx} + u_{yy} = f(x, y), \quad \Omega \subset (0,1)^2, \quad u_{\text{ex}}(x,y) = y^2 \sin(\pi x),\ \textit{The boundary of the domain is parameterized in polar form by}\ r(\theta) = R(1 + \alpha \cos k\theta),\ \textit{centred at}\ (0.5, 0.5), \textit{where}\ R = 0.40, \alpha = 0.15, \textit{and}\ k = 5$$

Dirichlet boundary conditions on all 4 sides

Configurations (N, Nc, Nb) = (289, 3618, 400)

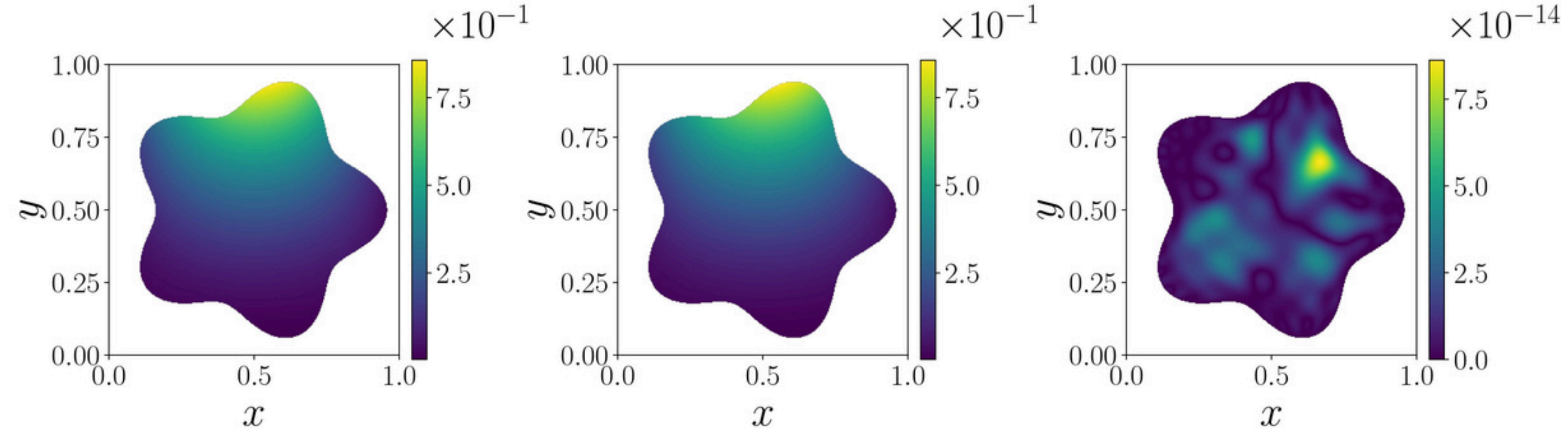

(a) Exact (b) LM – PIELM (Aug.) (c) Absolute Error

LM-PIELM (Aug.) solution plots

Case	Method	$\lVert u_{\text{ex}} - \hat{u} \rVert_\infty$	$\lVert \Phi_b \mathbf{C} - \mathbf{g} \rVert_\infty$
Star Domain	PIELM	1.49×10^{-12}	1.49×10^{-12}
	LM-PIELM	6.47×10^{-11}	2.92×10^{-11}
	LM-PIELM (Aug.)	$\mathbf{4.50 \times 10^{-14}}$	$\mathbf{1.33 \times 10^{-15}}$

Comparison table across different frameworks

- The algebraic formulation remains unchanged. Only the collocation and boundary points sampling locations modified
- No X-TFC comparison reported since the constrained expressions are not readily available for this geometry
- PIELM performs for this smooth elliptical problem, achieving relatively small solution and boundary errors, but LM-PIELM (Aug.) further improves the errors, reaching up to near machine precision levels as shown in the table above
- As we can see in the above figure, the numerical solution remains visually indistinguishable from the exact solution, and no noticeable artefacts appear near the curved boundary segments
- The same formulation, thus, can be easily extended to irregular geometries without any structural modifications

1D Unsteady Advection-Diffusion

$$u_t(x,t) + c\,u_x(x,t) - \kappa\,u_{xx}(x,t) = f(x,t), \quad (x,t) \in [0,1] \times [0,1],$$

with advection speed c = 1.0 and diffusion coefficient κ = 0.05. The exact solution is chosen as

$$u_{\text{ex}}(x,t) = \sin\big(2\pi(x - ct)\big)\, e^{-\alpha t}, \quad \alpha = 0.5,$$ Dirichlet boundary conditions on all sides

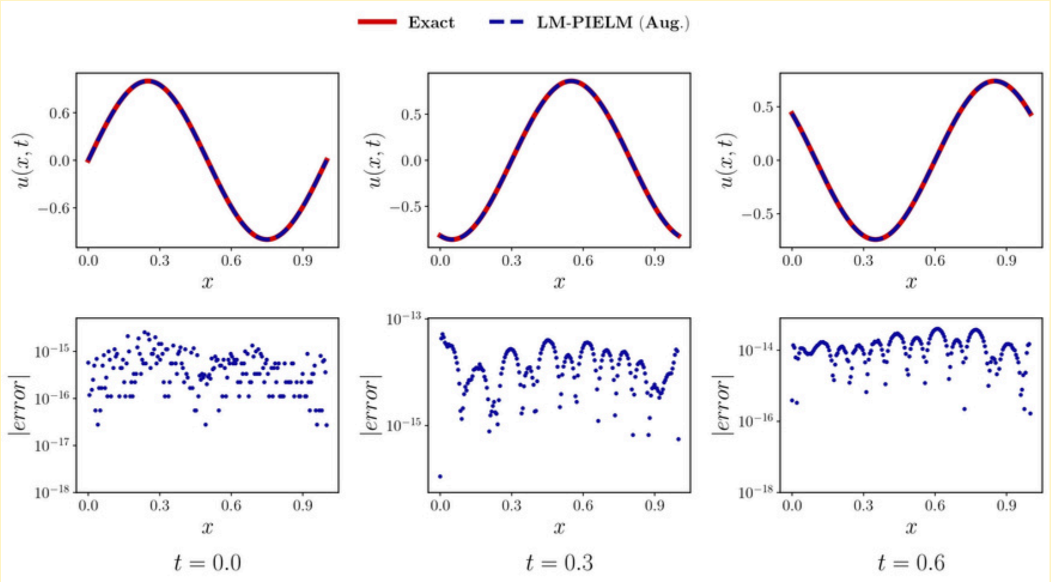

t	Method	$\|u_{\text{ex}} - \hat{u}\|_\infty$	$\|\Phi_b\mathbf{C} - \mathbf{g}\|_\infty$
0.0	LM-PIELM	6.00×10^{-14}	5.08×10^{-14}
	LM-PIELM (Aug.)	2.78×10^{-15}	5.88×10^{-16}
0.3	LM-PIELM	1.26×10^{-10}	4.88×10^{-15}
	LM-PIELM (Aug.)	5.20×10^{-14}	4.44×10^{-16}
0.6	LM-PIELM	1.05×10^{-10}	1.61×10^{-15}
	LM-PIELM (Aug.)	4.02×10^{-14}	2.77×10^{-16}

- This example demonstrates that the LM-PIELM formulation does not distinguish between spatial and temporal constraints, but instead treats all conditions through the same unified constrained system
- **Configuration:** N = 484 (22 x 22), Nc = 4692 (from 70 x 70 grid), Nb = 208, wall clock time (
- Across all timestamps demonstrated in the table, LM-PIELM (Aug.) consistently achieves solution error in order of 10^{-14} to 10^{-15} , while reducing boundary errors to machine precision

Results and Discussion

Inverse Problems

Inverse Diffusivity Identification in 1D Advection-Diffusion

Problem setup

$$u_x - \nu u_{xx} = f(x),\ \nu_{\text{true}} = 0.1$$

$$\Psi(\nu) = \Psi_{\text{adv}} - \nu\Psi_{\text{diff}}$$

- The parameter ν is then recovered through a one-dimensional Brent search method over the interval ν ∈ [10^{-3}, 0.9]
- **Configuration:** (N, Nc) = (25, 1000)

Results

		LM-PIELM		LM-PIELM (Aug.)	
M	η	$\frac{\lvert\nu_{\text{rec}}-\nu_{\text{true}}\rvert}{\lvert\nu_{\text{true}}\rvert}$	$\lVert\Phi_b\mathbf{C}-\mathbf{g}\rVert_\infty$	$\frac{\lvert\nu_{\text{rec}}-\nu_{\text{true}}\rvert}{\lvert\nu_{\text{true}}\rvert}$	$\lVert\Phi_b\mathbf{C}-\mathbf{g}\rVert_\infty$
5	0%	7.60×10^{-10}	2.22×10^{-16}	7.60×10^{-10}	2.22×10^{-16}
100	0%	4.51×10^{-9}	4.44×10^{-16}	4.51×10^{-9}	6.66×10^{-16}
20	1%	6.10×10^{-3}	5.55×10^{-16}	6.10×10^{-3}	4.44×10^{-16}
200	1%	6.62×10^{-4}	4.44×10^{-16}	6.62×10^{-3}	4.44×10^{-16}
50	5%	2.31×10^{-2}	4.44×10^{-16}	2.31×10^{-2}	2.22×10^{-16}
100	5%	9.26×10^{-5}	2.22×10^{-16}	9.26×10^{-3}	1.08×10^{-16}

- In the noiseless setting, both LM-PIELM formulations recover ν with relative errors of order 10^{-9}
- At larger noise levels, the L_infinity errors for ν remains stable, below 10^{-2}
- Across all sensor counts and noise levels, the boundary residual remains at approximately 10^{-15} to 10^{-16} for both LM-PIELM and LM-PIELM (Aug.).
- Thus, boundary enforcement mechanism remains decoupled from the parameter-identification process itself

Inverse Source Recovery on Star-Shaped Domain (2D Poisson)

Problem setup

- The setup remains same as that of the similar problem that was discussed earlier in the forward section
- Here, we aim to recover the source term "f"
- Dirichlet boundary conditions are imposed on the full boundary through, $u = u_{\text{ex}} \quad \text{on } \partial\Omega$
- **Configuration:** (N, Nc, Nb) = (169, 2420, 400)

Results

		LM-PIELM		LM-PIELM (Aug.)	
M	η	$\frac{\lVert \mathbf{f}_{\text{ex}} - \hat{\mathbf{f}} \rVert_2}{\lVert \mathbf{f}_{\text{ex}} \rVert_2}$	$\lVert \Phi_b \mathbf{C} - \mathbf{g} \rVert_\infty$	$\frac{\lVert \mathbf{f}_{\text{ex}} - \hat{\mathbf{f}} \rVert_2}{\lVert \mathbf{f}_{\text{ex}} \rVert_2}$	$\lVert \Phi_b \mathbf{C} - \mathbf{g} \rVert_\infty$
50	0%	2.89×10^{-3}	1.33×10^{-15}	5.23×10^{-4}	9.99×10^{-16}
500	0%	9.34×10^{-5}	9.99×10^{-16}	9.93×10^{-6}	9.99×10^{-16}
200	1%	1.01×10^{0}	1.92×10^{-11}	1.01×10^{0}	1.92×10^{-11}
1000	1%	6.36×10^{-1}	4.06×10^{-11}	6.35×10^{-1}	7.04×10^{-12}
200	5%	8.43×10^{-1}	1.60×10^{-11}	8.44×10^{-1}	1.57×10^{-11}
500	5%	5.87×10^{-1}	2.16×10^{-11}	5.87×10^{-1}	2.01×10^{-11}

- The same constrained algebraic framework used for the forward problem is retained without structural modification
- Tikhonov regularization is used since source recovery is substantially more sensitive to noise
- In the noiseless setting, both constrained formulations recover the source term accurately
- Under noisy measurements, the source reconstruction error increases significantly for both methods
- Nevertheless, even in these more challenging settings, the boundary residual remains small across all configurations

Additional Inverse Problems

Conductivity identification: 1D Heat Conduction

		LM-PIELM			LM-PIELM (Aug.)		
M	η	$\frac{\lvert\kappa_{\text{rec}}-\kappa_{\text{true}}\rvert}{\lvert\kappa_{\text{true}}\rvert}$	$\lVert T_{\text{ex}}-\hat{T}\rVert_\infty$	$\lVert\Phi_b\mathbf{C}-\mathbf{g}\rVert_\infty$	$\frac{\lvert\kappa_{\text{rec}}-\kappa_{\text{true}}\rvert}{\lvert\kappa_{\text{true}}\rvert}$	$\lVert T_{\text{ex}}-\hat{T}\rVert_\infty$	$\lVert\Phi_b\mathbf{C}-\mathbf{g}\rVert_\infty$
5	0%	1.39×10^{-9}	1.74×10^{-10}	5.83×10^{-17}	1.39×10^{-9}	1.74×10^{-10}	4.04×10^{-16}
10	0%	1.39×10^{-9}	1.74×10^{-10}	5.03×10^{-17}	1.39×10^{-9}	1.75×10^{-10}	2.19×10^{-16}
20	0%	1.39×10^{-9}	1.74×10^{-10}	7.13×10^{-17}	1.40×10^{-9}	1.75×10^{-10}	2.89×10^{-17}
50	0%	1.40×10^{-9}	1.75×10^{-10}	7.26×10^{-17}	1.40×10^{-9}	1.75×10^{-10}	1.62×10^{-16}
100	0%	1.41×10^{-9}	1.76×10^{-10}	3.64×10^{-17}	1.41×10^{-9}	1.76×10^{-10}	4.64×10^{-17}
200	0%	1.42×10^{-9}	1.77×10^{-10}	3.29×10^{-17}	1.42×10^{-9}	1.78×10^{-10}	2.98×10^{-16}
5	1%	8.36×10^{-4}	1.04×10^{-4}	4.33×10^{-17}	4.41×10^{-3}	5.54×10^{-4}	1.58×10^{-16}
10	1%	2.16×10^{-3}	2.71×10^{-4}	9.88×10^{-17}	1.45×10^{-3}	1.81×10^{-4}	1.63×10^{-16}
20	1%	8.47×10^{-4}	1.06×10^{-4}	1.42×10^{-16}	2.58×10^{-3}	3.22×10^{-4}	5.20×10^{-16}
50	1%	3.10×10^{-3}	3.86×10^{-4}	1.39×10^{-17}	3.78×10^{-4}	4.72×10^{-5}	3.37×10^{-16}
100	1%	8.10×10^{-4}	1.01×10^{-4}	2.19×10^{-17}	1.55×10^{-4}	1.93×10^{-5}	7.63×10^{-17}
200	1%	7.39×10^{-4}	9.24×10^{-5}	8.67×10^{-17}	1.20×10^{-3}	1.49×10^{-4}	5.19×10^{-16}
5	5%	6.09×10^{-3}	7.66×10^{-4}	6.97×10^{-17}	2.23×10^{-2}	2.85×10^{-3}	2.74×10^{-16}
10	5%	1.37×10^{-2}	1.74×10^{-3}	3.64×10^{-17}	5.52×10^{-3}	6.86×10^{-4}	1.54×10^{-16}
20	5%	2.44×10^{-3}	3.06×10^{-4}	1.57×10^{-17}	1.48×10^{-2}	1.82×10^{-3}	2.36×10^{-16}
50	5%	1.70×10^{-2}	2.16×10^{-3}	3.12×10^{-17}	4.45×10^{-3}	5.59×10^{-4}	4.49×10^{-16}
100	5%	5.01×10^{-3}	6.23×10^{-4}	6.53×10^{-17}	1.58×10^{-3}	1.98×10^{-4}	3.57×10^{-16}
200	5%	4.48×10^{-3}	5.58×10^{-4}	5.67×10^{-17}	8.01×10^{-4}	1.00×10^{-4}	2.24×10^{-16}

- **Configuration:** (N, Nc) = (25, 1000)

$$-\kappa T_{xx} = 1,\ \kappa_{\text{true}} = 1.0,\ T(x) = \frac{x(1-x)}{2\kappa}$$

Source Recovery in 2D Helmholtz

k = π

		LM-PIELM		LM-PIELM (Aug.)	
M	η	$\frac{\lVert\mathbf{f}_{\text{ex}}-\hat{\mathbf{f}}\rVert_2}{\lVert\mathbf{f}_{\text{ex}}\rVert_2}$	$\lVert\Phi_b\mathbf{C}-\mathbf{g}\rVert_\infty$	$\frac{\lVert\mathbf{f}_{\text{ex}}-\hat{\mathbf{f}}\rVert_2}{\lVert\mathbf{f}_{\text{ex}}\rVert_2}$	$\lVert\Phi_b\mathbf{C}-\mathbf{g}\rVert_\infty$
50	0%	1.86×10^{-1}	5.43×10^{-17}	1.86×10^{-1}	1.09×10^{-16}
100	0%	1.96×10^{-3}	1.27×10^{-16}	1.96×10^{-3}	1.70×10^{-16}
200	0%	1.70×10^{-6}	1.61×10^{-16}	1.86×10^{-6}	2.67×10^{-16}
500	0%	3.37×10^{-8}	4.26×10^{-16}	3.77×10^{-8}	1.89×10^{-16}
1000	0%	2.52×10^{-8}	7.21×10^{-16}	1.47×10^{-8}	3.68×10^{-16}
50	1%	9.45×10^{-1}	7.20×10^{-17}	9.45×10^{-1}	1.09×10^{-16}
100	1%	6.96×10^{-1}	4.99×10^{-17}	6.96×10^{-1}	1.34×10^{-16}
200	1%	6.51×10^{-1}	1.24×10^{-16}	6.51×10^{-1}	1.80×10^{-16}
500	1%	5.17×10^{-1}	6.06×10^{-16}	5.17×10^{-1}	3.99×10^{-16}
1000	1%	4.51×10^{-1}	1.07×10^{-15}	4.51×10^{-1}	6.86×10^{-16}
50	5%	2.75×10^{0}	7.76×10^{-17}	2.75×10^{0}	6.92×10^{-17}
100	5%	2.02×10^{0}	4.65×10^{-17}	2.02×10^{0}	2.84×10^{-16}
200	5%	2.49×10^{0}	1.56×10^{-16}	2.49×10^{0}	2.55×10^{-16}
500	5%	2.34×10^{0}	5.73×10^{-16}	2.34×10^{0}	5.06×10^{-16}
1000	5%	1.80×10^{0}	1.15×10^{-15}	1.80×10^{0}	3.17×10^{-16}

k = 1

		LM-PIELM		LM-PIELM (Aug.)	
M	η	$\frac{\lVert\mathbf{f}_{\text{ex}}-\hat{\mathbf{f}}\rVert_2}{\lVert\mathbf{f}_{\text{ex}}\rVert_2}$	$\lVert\Phi_b\mathbf{C}-\mathbf{g}\rVert_\infty$	$\frac{\lVert\mathbf{f}_{\text{ex}}-\hat{\mathbf{f}}\rVert_2}{\lVert\mathbf{f}_{\text{ex}}\rVert_2}$	$\lVert\Phi_b\mathbf{C}-\mathbf{g}\rVert_\infty$
50	0%	1.89×10^{-1}	5.20×10^{-17}	1.89×10^{-1}	7.09×10^{-17}
100	0%	1.40×10^{-3}	1.15×10^{-16}	1.40×10^{-3}	1.32×10^{-16}
200	0%	2.76×10^{-5}	1.06×10^{-16}	2.76×10^{-5}	3.08×10^{-16}
500	0%	4.17×10^{-8}	2.25×10^{-16}	2.94×10^{-8}	3.10×10^{-16}
1000	0%	1.37×10^{-8}	9.35×10^{-16}	8.92×10^{-9}	8.57×10^{-16}
50	1%	7.07×10^{-1}	5.58×10^{-17}	7.07×10^{-1}	9.91×10^{-17}
100	1%	3.36×10^{-1}	7.44×10^{-17}	3.36×10^{-1}	2.63×10^{-16}
200	1%	2.79×10^{-1}	1.18×10^{-16}	2.79×10^{-1}	1.98×10^{-16}
500	1%	2.16×10^{-1}	3.86×10^{-16}	2.16×10^{-1}	7.31×10^{-16}
1000	1%	3.11×10^{-1}	8.30×10^{-16}	3.11×10^{-1}	6.14×10^{-16}
50	5%	1.85×10^{0}	3.14×10^{-17}	1.85×10^{0}	1.13×10^{-16}
100	5%	9.78×10^{-1}	9.05×10^{-17}	9.78×10^{-1}	6.79×10^{-17}
200	5%	1.24×10^{0}	1.55×10^{-16}	1.24×10^{0}	2.19×10^{-16}
500	5%	1.80×10^{0}	2.95×10^{-16}	1.80×10^{0}	3.89×10^{-16}
1000	5%	1.04×10^{0}	9.12×10^{-16}	1.04×10^{0}	4.34×10^{-16}

- **Configuration:** (N, Nc, Nb) = (225, 7396, 348)

$u_{xx} + u_{yy} + k^2 u = f,$ *posed on the unit square domain* $(0,1)^2$

The exact solution is $u(x,y) = \sin(\pi x)\sin(\pi y)$

- Boundary errors consistently confined to the orders of 10^{-16} - 10^{-17} irrespective of sensor count and noise levels

Conclusion

- Proposed LM-PIELM framework with **hard boundary enforcement using Lagrange multipliers** instead of soft penalty terms
- Converts constrained PDE learning problem into a **structured linear saddle-point system**, avoiding iterative nonlinear optimization
- **Unified algebraic framework** for Dirichlet, Neumann, and mixed boundary conditions without geometry-specific modifications
- **Developed an augmented-system formulation** avoiding explicit Gram matrix formation, improving numerical stability in ill-conditioned cases
- Achieved **near machine-precision boundary satisfaction** across forward and inverse problems
- Demonstrated robustness on advection-dominated, irregular-domain, and unsteady space-time problems
- Naturally extends to inverse parameter and source reconstruction problems while preserving boundary admissibility independently of reconstruction quality

Future Works

Extension to:

- moving-boundary cases
- interface
- multiphysics
- coupled-PDEs

THANK YOU !